Journal of Global Change Data & Discovery. 2021, 5(2): 162-174
www.geodoi.ac.cn

Standardized Anomaly Dataset of Global Marine Net Primary Productivity (1998–2019)

Sun, Y. Q.[1, 2] Xue, C. J.[2, 3*] Hong, Y. L.[4] Xu, Y. F.[2,5] Liu, J. Y.[2,6]

1. China University of Geosciences, Beijing 100083, China;
2. China Aerospace Information Research Institute Chinese Academy of Sciences, Beijing 100094, China;
3. China Key Laboratory of Digital Earth Science, Aerospace Information Research Institute, Chinese Academy of Sciences, Beijing 100094, China;
4. China Multidisciplinary Digital Publishing Institute, Beijing 101100, China;
5. China University of Petroleum, Qingdao 266580, China;
6. China CETC Key Laboratory of Aerospace Information Applications, Shi Jiazhuang 050081, China

Abstract: Marine net primary production (MNPP) is an important parameter in marine ecosystems and is an indicator that measures the photosynthesis capacity of marine phytoplankton. The temporal and spatial characteristics of its abnormal change patterns are related to global climate change, the carbon cycle, and the global ecological environment, which have close ties. This article uses the SeaWiFS.R2014 version from January 1998 to December 2002 and the MODIS. R2018 version from January 2003 to December 2019 as provided by the Ocean Productivity website of Oregon State University as the original data. The spatiotemporal statistical analysis methods have developed a global ocean primary productivity standardized anomaly dataset on three time scales from 1998 to 2019: yearly, quarterly, and monthly. The dataset has a spatial resolution of 9 km × 9 km and a temporal resolution of 9 km × 9 km. For the month category, the data format is HDF4 with a volume of 16.82 GB (4.81 GB after compression). This paper uses the multiple El Niño-Southern Oscillation (ENSO) index (MEI) to initially analyze the coupling relationship between the abnormal change pattern of the marine primary productivity and the ENSO event. The results show that the evolutions of the abnormal change pattern of marine primary productivity and the occurrence and disappearance of ENSO events are closely related, which proves the feasibility and validity of the global ocean primary productivity standardized anomaly dataset.

Keywords: Marine primary productivity; abnormal change; monthly mean anomaly; seasonal mean anomaly; annual mean anomaly

DOI: https://doi.org/10.3974/geodp.2021.02.08
CSTR: https://cstr.escience.org.cn/CSTR:20146.14.2021.02.08

Dataset Availability Statement:

The dataset supporting this paper was published and is accessible through the *Digital Journal of Global Change Data Repository* at: https://doi.org/10.3974/geodb.2020. 2020.07.13.V1 or https://cstr.escience.org.cn/CSTR:20146.11.2020.07.13.V1.

Received: 02-02-2021; **Accepted:** 02-04-2021; **Published:** 25-06-2021

Foundations: Chinese Academy of Sciences (XDA19060103); Ministry of Science and Technology of P. R. China (2017YFB0503605); National Natural Science Foundation of China (41671401)

***Corresponding Author:** Xue, C. J. 0000-0003-3605-6578, Aerospace Information Research Institute, Chinese Academy of Sciences, xuecj@aircas.ac.cn

Data Citation: [1] Sun, Y. Q., Xue, C. J., Hong, Y. L., *et al*. Standardized anomaly dataset of global marine net primary productivity (1998–2019) [J]. *Journal of Global Change Data & Discovery*, 2021, 5(2): 162–174. https://doi.org/10.3974/geodp.2021.02.08. https://cstr.escience.org.cn/CSTR:20146.14.2021.02.08.
[2] Sun, Y. Q., Xue, C. J., Hong, Y. L., *et al*. Standardized anomaly dataset of global marine net primary productivity (1998–2019) [J/DB/OL]. *Digital Journal of Global Change Data Repository*, 2020. https://doi.org/10.3974/geodb.2020.07.13.V1. https://cstr.escience.org.cn/CSTR:20146.11.2020.07.13.V1.

1 Introduction

The marine net primary production (MNPP) is the photosynthesis capacity of marine phytoplankton per unit area[1]. This is an important parameter in marine ecosystems as it helps to understand the global carbon cycle, fishery production capacity, etc.[2]. The application of satellite remote sensing technology provides new possibilities to study MNPP. Satellite remote sensing has the characteristics of a large coverage area and long observation time series, making it an indispensable tool to measure and research marine phytoplankton abundance at large time and space scales. The MNPP has abnormal changes in time and space in the average state of a long time series at a certain time, which can occur at the monthly, seasonal, annual, etc. scales[3]. Abnormal changes in the MNPP and the associated relationship with marine environmental elements have different temporal and spatial distribution characteristics[4]. The abnormal change patterns of MNPP and the correlation patterns with marine environmental elements provide a basis to clarify the primary influencing factors on the temporal and spatial distributions of phytoplankton, while at the same time providing a basis to study how climate change affects the marine food web[5]. In addition, abnormal changes in the MNPP are also closely related to El Niño-Southern Oscillation (ENSO) events[6]. For example, Bastos *et al*. found that there is a strong anti-correlation between the ENSO and MNPP, which is driven primarily by ecosystems in tropical and subtropical latitudes[7]. Chavez *et al*. found that during the occurrence of ENSO, MNPP increased significantly in tropical regions due to the influences of upwelling and nutrient supply[8]. Therefore, it is significant to research abnormal changes in the MNPP[9]. Although there are a variety of MNPP datasets based on satellite remote sensing, such as GlobalMarineABMP_NPP[10], Chlorophyll-a Concen of Poyang Lake, China[11], and MuSyQ-NPP-1km-2013[12], there are no relevant reports on spatiotemporal datasets.

This paper is based on the existing monthly average MNPP dataset (1998.01–2019.12) using geographic temporal and spatial statistical analysis methods. This work considers the temporal and spatial characteristics of marine primary productivity and designs the production method for the MNPP abnormal change dataset to remove seasonal variations. Thus, standardized anomaly datasets of marine primary productivity on annual, seasonal, and monthly time scales are generated (MNPP monthly anomaly datasets, MNPP-MAD; MNPP seasonal anomaly datasets, MNPP-SAD; MNPP annual anomaly datasets, MNPP-AAD). This dataset provides a basis for global climate change research.

2 Metadata of the Dataset

The metadata of the Standardized anomaly dataset of global marine net primary productivity (1998–2019)[13] is summarized in Table 1. It includes the dataset full name, short name, authors, year of the dataset, temporal resolution, spatial resolution, data format, data size, data files, data publisher, and data sharing policy, etc.

3 Data Development Method

3.1 Data Sources

The NPP data in this article from January 1998 to December 2002 are derived from the data of Sea-Viewing Wide Field-of-View Sensor (SeaWiFS) satellite platform R2014 based on the SeaWiFS CHL, AVHRR SST, and SeaWiFS photosynthetic radiation (PAR) data. The

data are calculated using the vertical generalized production model (VGPM) algorithm[15]. The NPP data from January 2003 to December 2019 are derived from the Moderate Resolution Imaging Spectroradiometer (MODIS) sensor on the Aqua satellite platform, and the data version is R2018. This dataset is based on MODIS CHL, MODIS SST, and MODIS PAR. The data were calculated using the VGPM model algorithm, and the NPP data for the two

Table 1 Metadata summary of Standardized anomaly dataset of global marine net primary productivity (1998–2019)

Item	Description
Dataset name	Standardized anomaly dataset of global marine net primary productivity (1998–2019)
Dataset short name	Global_MNPP_Anomaly_1998-2019
Authors	Sun, Y. Q., China University of Geosciences, Beijing, Aerospace Information Research Institute, Chinese Academy of Sciences, syqsdkd@126.com Xue, C. J. 0000-0003-3605-6578, Aerospace Information Research Institute, Chinese Academy of Sciences, Key Laboratory of Digital Earth Science, Aerospace Information Research Institute, Chinese Academy of Sciences, xuecj@aircas.ac.cn Hong, Y. L., Multidisciplinary Digital Publishing Institute, Beijing, 515251357@qq.com Xu ,Y. F., China University of Petroleum，Qingdao, Aerospace Information Research Institute, Chinese Academy of Sciences, xuyf187627@163.com Liu, J. Y., CETC Key Laboratory of Aerospace Information Applications, liujy@aircas.ac.cn
Geographical region	Global waters Year From January 1998 to December 2019
Temporal resolution	Month, season, year
Spatial resolution	9 km × 9 km Data format HDF4
Data size	16.82 GB (After compression 4.81 GB)
Data files	The dataset consists of six sub-datasets, which are described as follows: (1) Original dataset of the global ocean primary productivity year (2) Seasonal raw datasets of the global ocean primary productivity (3) Monthly raw dataset of the global ocean primary productivity (4) Monthly standardized dataset of the global ocean primary productivity (5) Dataset for seasonally standardized anomalies of the global marine primary productivity (6) Global Ocean Primary Productivity Annual Standardized Anomaly Dataset
Foundations	Strategic Type A Pilot Special Project of the Chinese Academy of Sciences (XDA19060103); National Key R&D Program Project (2017YFB0503605); and National Natural Science Foundation of China (41671401)
Data publisher	Global Change Research Data Publishing &Repository http://www.geodoi.ac.cn
Address	No. 11, Datun Road, Chaoyang District, Beijing 100101
Data sharing policy	***Data*** from the Global Change Research Data Publishing & Repository includes metadata, datasets (in the *Digital Journal of Global Change Data Repository*), and publications (in the *Journal of Global Change Data & Discovery*). ***Data*** sharing policy includes: (1) ***Data*** are openly available and can be free downloaded via the Internet; (2) End users are encouraged to use ***Data*** subject to citation; (3) Users, who are by definition also value-added service providers, are welcome to redistribute ***Data*** subject to written permission from the GCdataPR Editorial Office and the issuance of a ***Data*** redistribution license; and (4) If ***Data*** are used to compile new datasets, the 'ten per cent principal' should be followed such that ***Data*** records utilized should not surpass 10% of the new dataset contents, while sources should be clearly noted in suitable places in the new dataset[14]
Communication and searchable system	DOI, CSTR, Crossref, DCI, CSCD, CNKI, SciEngine, WDS/ISC, GEOSS

periods were provided by the Oregon State University Ocean Productivity Website (http://www.science.oregonstate.edu/ocean.productivity)[6]. The data time resolution is monthly, the spatial resolution is 9 km × 9 km, and the global grid number is 2160×4320.

3.2 Algorithm Flow

For the data obtained by the two sensors, SeaWiFS and MODIS, Couto *et al*. conducted correlation and standard deviation analyses. The results show that the two datasets can be combined and the results are not affected by sensor conversion[16]. Therefore, this paper uses

the MNPP dataset from the two sensors as the original input data. First, the original data was spatially converted, and the longitude range of the original data was converted from –180°–180° to 0°–360° and was processed using time interpolation and time aggregation algorithms to obtain the original data for the seasonal and annual scales. The time interpolation algorithm fills in bad data by taking invalid grid values at a certain time and filling them in with the average of those at the same location at adjacent times (previous and next). The time aggregation algorithm, taking spring as an example, averages the data for March, April, and May to generate the corresponding seasonal scale data. For annual scale data, the data from January to December of each year are averaged. As marine primary productivity has strong seasonal changes (shown in Figure 3), which is driven primarily by solar radiation, it conceals abnormal change patterns of the marine primary productivity. Thus, we study the abnormal changes in the MNPP data collection to eliminate these seasonal patterns. This paper adopts the standardized anomaly method called the Z-score to eliminate seasonal variation patterns in the marine primary productivity[17]. For any month from January to December, we obtain the value each year to form a time series and calculate its average and standard deviation. The mean and standard deviation are used to discretize the average monthly value over all years, as shown in equation (1)[18].

$$X'_{i,j} = \frac{X_{i,j} - \overline{Xj}}{\delta_j} \quad (\text{j=1,2,.....,12}) \tag{1}$$

where i is the year, j is the month, $\overline{X}_j$ and δ_j are the mean and standard deviation, respectively, and $X'_{i,j}$ and $X_{i,j}$ are the original and converted values of the long-term image series.

To verify the applicability of the MNPPAD dataset, this paper selects a typical MNPP cluster evolution model and analyzes its relationship with ENSO events, which indirectly proves the scientific nature of the dataset. The algorithm flow of the MNPPAD dataset is shown in Figure 1.

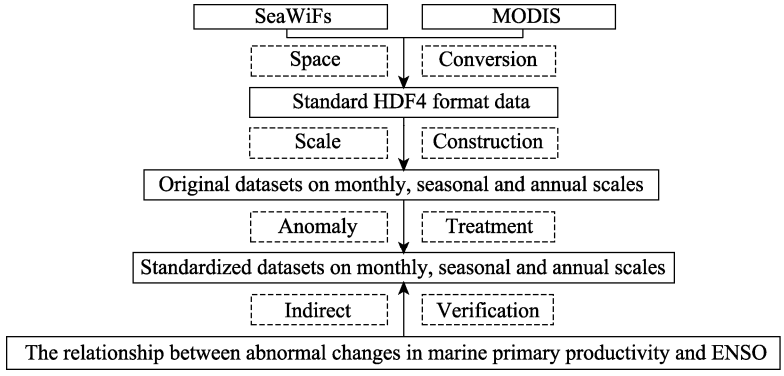

Figure 1 Technology roadmap

4 Data Result

4.1 Dataset Composition

The global ocean primary productivity dataset (1998–2019) includes raw and result data. The data format is HDF4, and its data structure is customized, as shown in Figure 2. The

data description module description is shown in Table 1, and the data elements and attributes are described in Table 2.

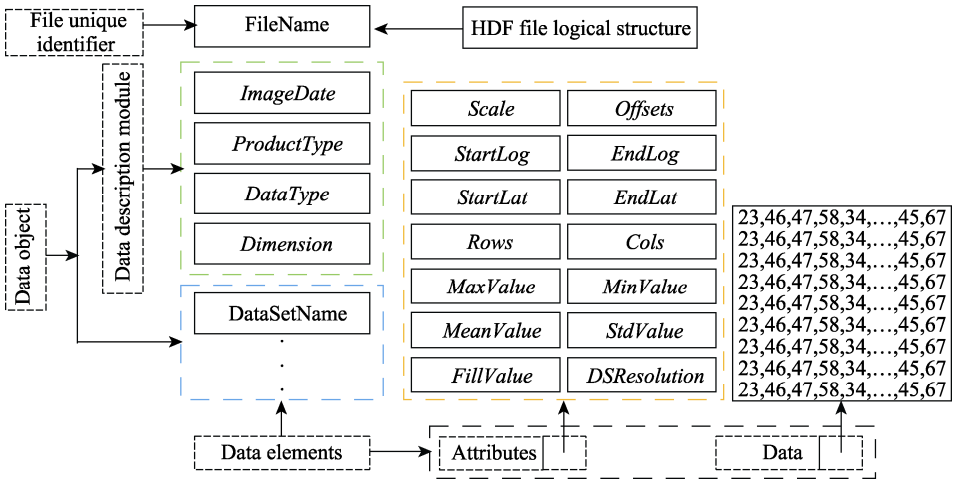

Figure 2 HDF4 data structure diagram

Table 1 HDF4 data description module table

Name	Definition	Comment
ImageDate	DFNT_CHAR8	Time of remote sensing image
ProductType	DFNT_CHAR8	Product type:the default is Product
DataType	DFNT_CHAR8	Data type:default is 0
Dimension	DFNT_CHAR8	Data dimension: the default is two-dimensional

Table 2 HDF4 data element and attribute description table

Name	Definition	Comment
DataSetName	DFNT_INT32	Dataset name
Scale	DFNT_FLOAT64	Scale factor: default is 0.001
Offsets	DFNT_FLOAT64	Scale intercept: default is 0
StartLog	DFNT_FLOAT64	Remote sensing image starting longitude
EndLog	DFNT_FLOAT64	Remote sensing image termination longitude
StartLat	DFNT_FLOAT64	Starting Latitude of remote sensing image
EndLat	DFNT_FLOAT64	Remote sensing image termination latitude
Rows	DFNT_UINT16	Number of rows of remote sensing image
Cols	DFNT_UINT16	Number of remote sensing images
MaxValue	DFNT_FLOAT64	Remote sensing image pixel maximum
MinValue	DFNT_FLOAT64	Remote sensing image pixel minimum
MeanValue	DFNT_FLOAT64	Remote sensing image pixel value average
StdValue	DFNT_FLOAT64	Standard deviation of remote sensing image pixel value
FillValue	DFNT_INT32	Filling value of remote sensing image: default is –9999
DSResolution	DFNT_FLOAT64	Remote sensing image spatial resolution

4.2 Data Preprocessing

Figure 3 compares the time series of the original marine primary productivity data and the anomalous data in global oceans from January 1998 to December 2019. The analysis of Figure 3 indicates that the standardized anomaly processing after removing the seasonal component of the original data better shows the volatility of the marine primary productivity in the time series. After the standardized anomaly processing, the spatial distribution map of the monthly average anomaly in the MNPP from Figure 4(b) shows the abnormally increased and decreased areas.

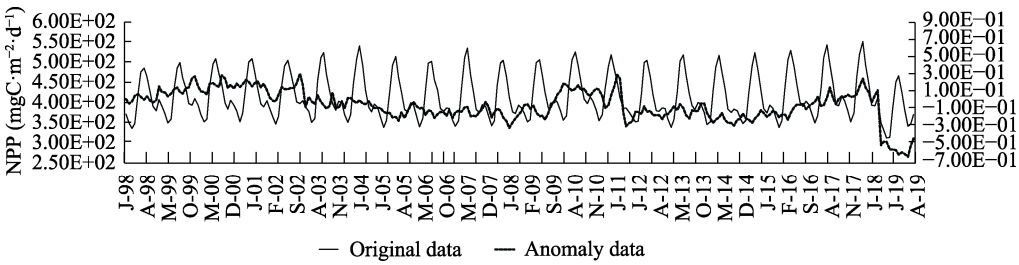

Figure 3 Comparison of the time series between the original marine primary productivity data and the anomaly data (January 1998–December 2019)

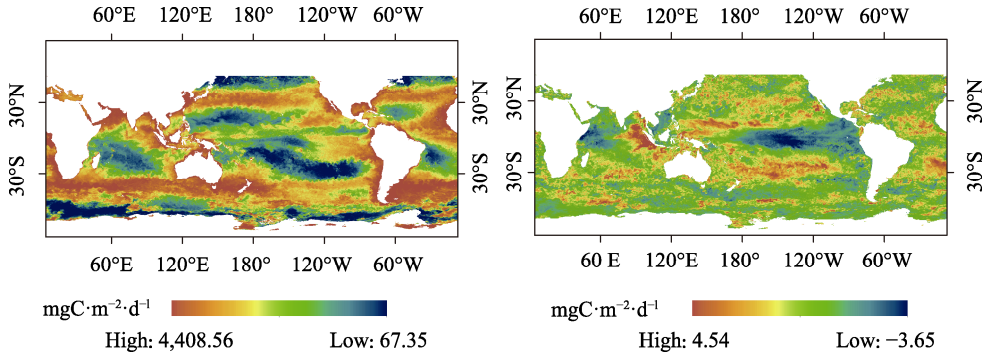

(a) Spatial distribution of MNPP

(b) Spatial distribution of standardized monthly mean anomalies of MNPP

Figure 4 Original MNPP data and monthly average standardized anomaly data in January 1998

4.3 Data Result

The data result include: (1) global ocean primary productivity annual standardized anomaly Dataset (see Figure 5 for an example); (2) global ocean primary productivity seasonal standardized anomaly dataset (see Figure 6 for an example); and (3) global ocean primary productivity annual standardized anomaly dataset (see Figure 6 for an example) (4) monthly standardized anomaly dataset for productivity (see Figure 7 for an example).

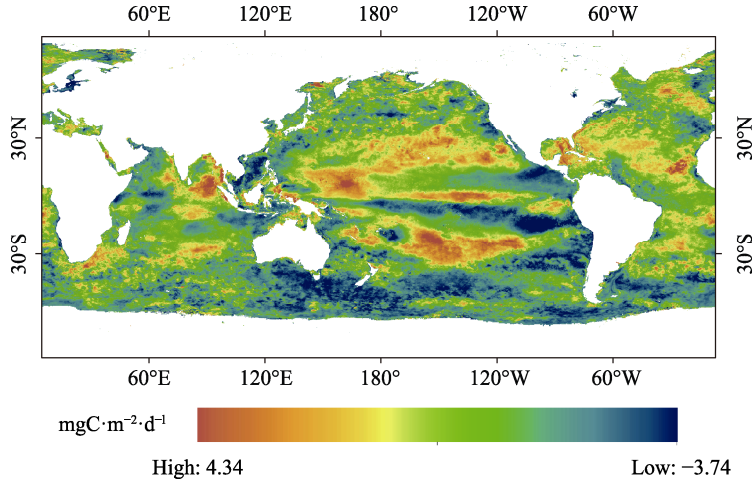

Figure 5 Annual average anomaly map of global marine primary productivity (1998–2019)

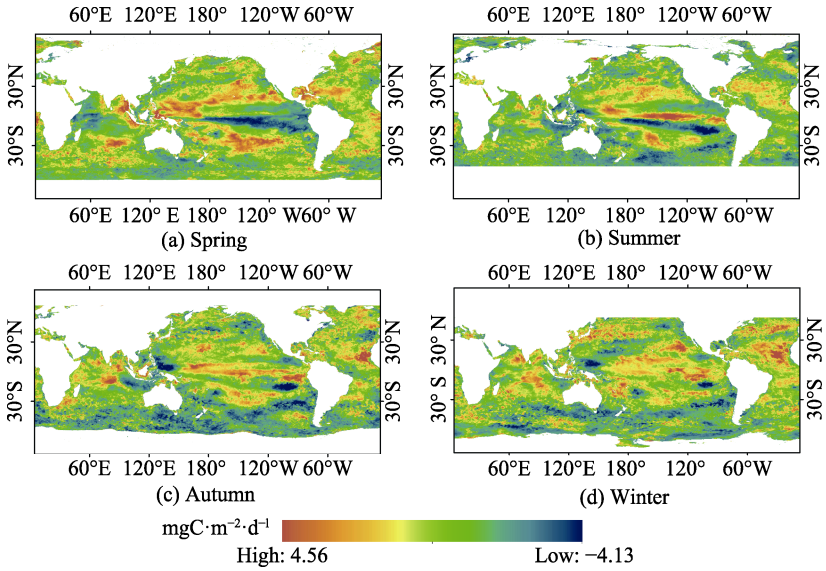

Figure 6 Data map of seasonal average anomalies for the global marine primary productivity (1998–2019)

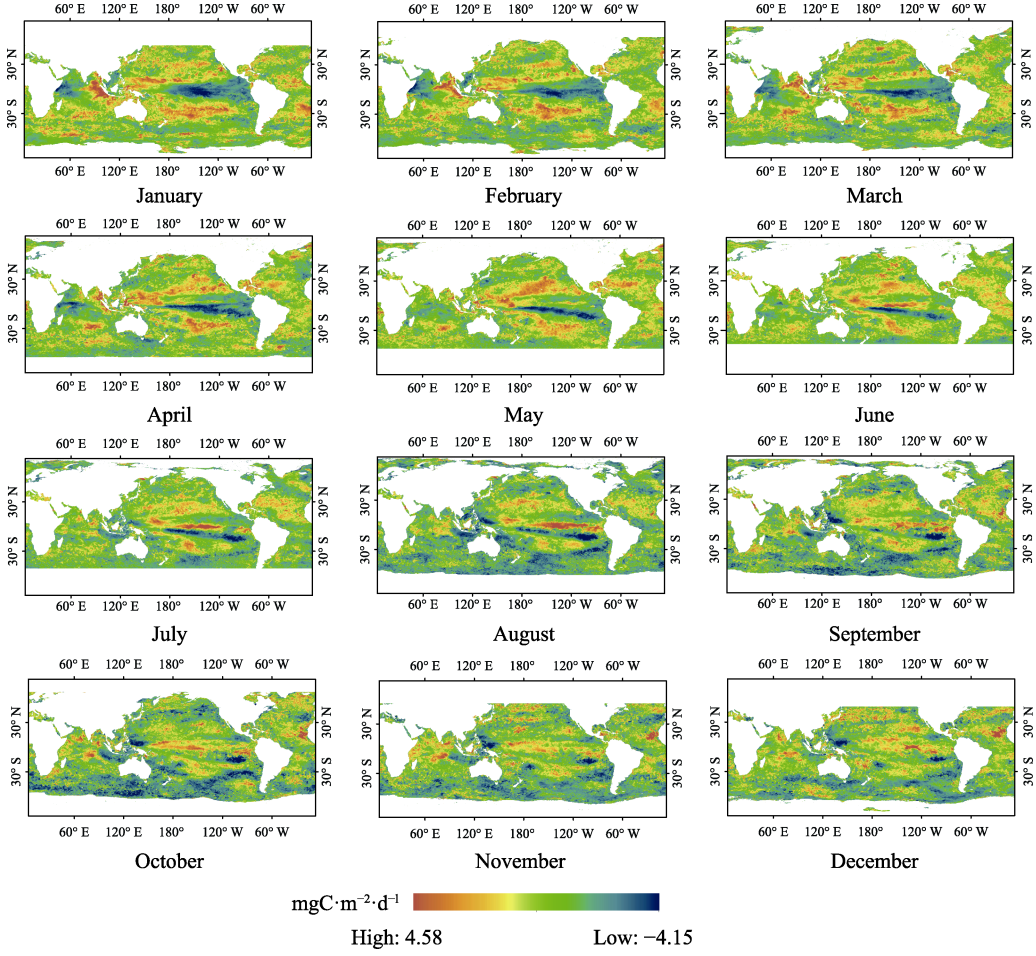

Figure 7 Data map of monthly average anomalies for the global marine primary productivity (1998–2019)

4.4 Dataset Suitability Verification

This paper uses the coupling relationship between the MEI and the abnormal change pattern of the marine primary productivity to indirectly verify the applicability of the MNPPAD dataset. The double-constrained clustering method developed by the subject[19] is used to extract the temporal and spatial cluster patterns of the primary productivity anomalies in the Pacific Ocean to analyze the El Niño event from January 1998 to July 1998 and the La Niña from December 1998 to August 1999. During the La Niña event, the El Niño event from August 2006 to February 2007, and the La Niña event from June 2010 to March 2011, the temporal and spatial cluster patterns of the ocean primary productivity anomalies in the Indian Ocean, equatorial Pacific, and Atlantic regions were mainly. The results are shown in Figures 8–15.

Figure 8 shows the spatial variations of the spatial and temporal clusters for the abnormally low marine primary productivity in the western Indian Ocean from January 1998 to July 1998. Over time, the position of the spatiotemporal cluster remained nearly unchanged, and the coverage area gradually decreased until disappearing. Figure 9 shows the correlation diagram between the area of the spatiotemporal cluster and MEI. It is seen that during El Niño, the spatiotemporal evolution cluster has a response relationship with the MEI index, and the correlation coefficient reaches 0.97.

Figure 10 shows the spatial variations of the spatial and temporal clusters of the abnormally high ocean primary productivity in the central and eastern equatorial Pacific from December 1998 to August 1999. Over time, the temporal and spatial anomalous high-value

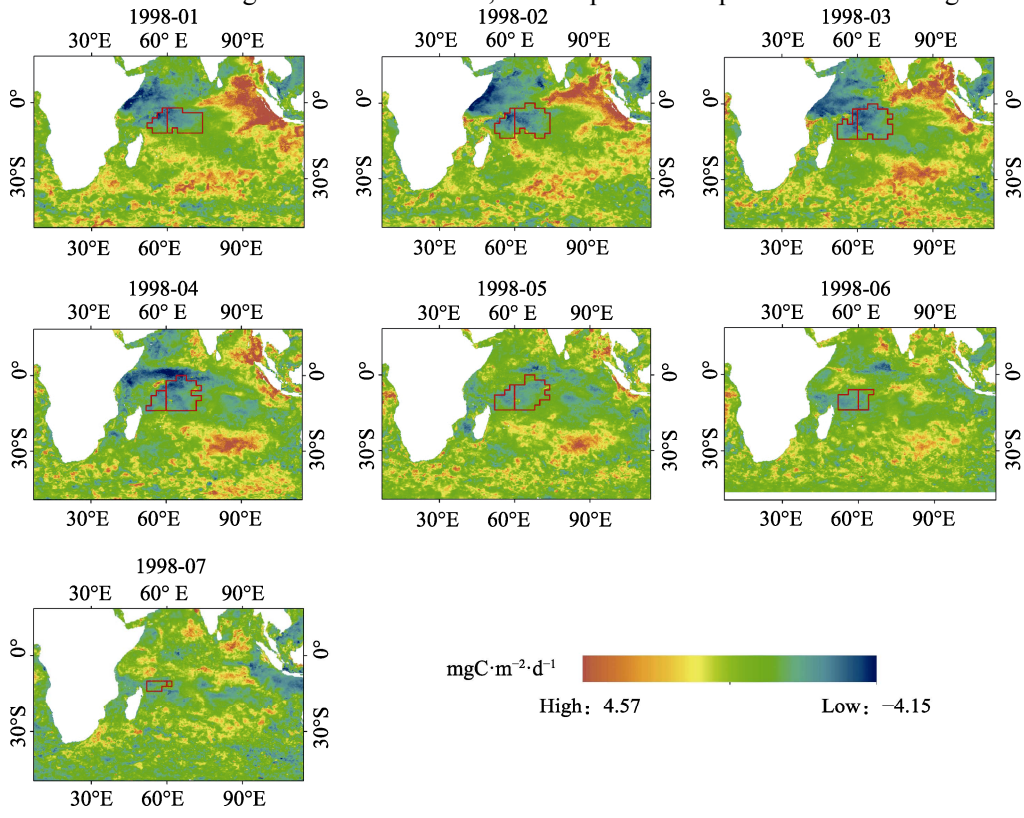

Figure 8 Spatial movement of anomalous low-value spatiotemporal clusters in the western Indian Ocean

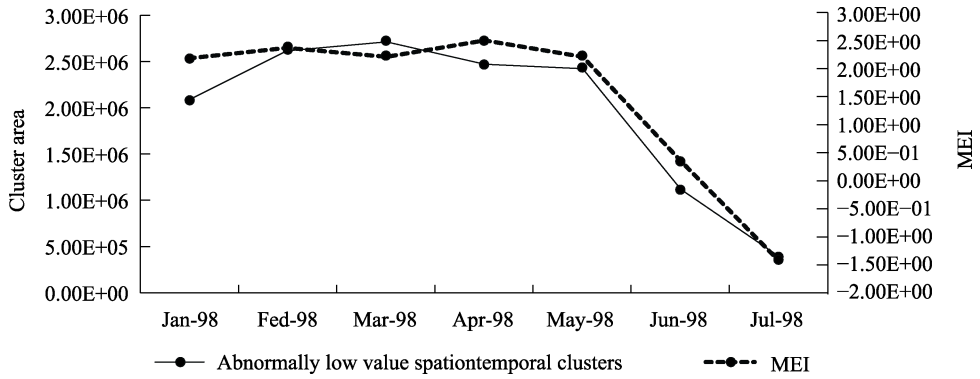

Figure 9 Correlation between the area of the spatiotemporal clusters and the MEI

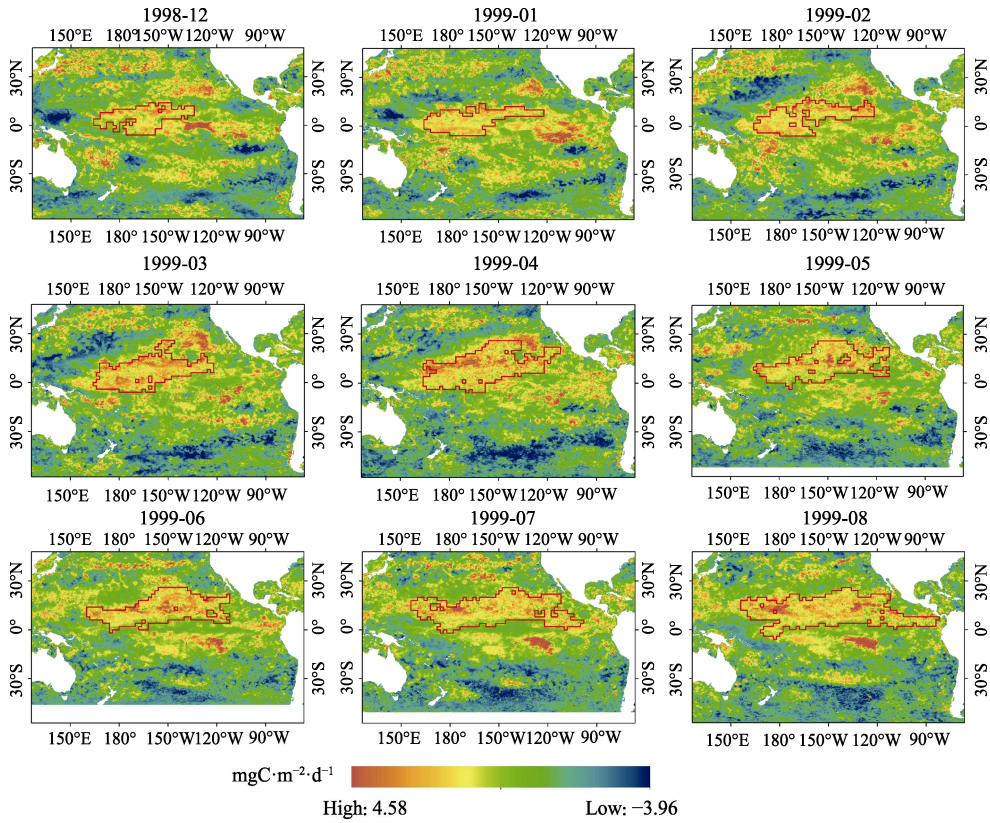

Figure 10 Spatial movement of anomalous high-value spatiotemporal clusters in the equatorial Central and Eastern Pacific

clusters gradually moved east, and the coverage area gradually increased. Figure 11 shows the correlation diagram between the spatiotemporal evolution cluster area and the MEI. It is seen that during La Niña, the spatiotemporal evolution cluster has a response relationship with the MEI index, and the correlation coefficient reaches 0.79.

Figure 12 shows the spatial variation in the spatial and temporal clusters of the abnormally low marine primary productivity in the central and southern equatorial Pacific Ocean from June 2006 to February 2007. Over time, the temporal and spatial anomalous low-value clusters gradually moved southeast, and the coverage area gradually became larger. Since

January 2007, the area gradually became smaller and disappeared. Figure 13 shows the correlation diagram between the area of the spatiotemporal evolution cluster and the MEI. It is seen that during El Niño, the spatiotemporal evolution cluster has a response relationship with the MEI index, and the correlation coefficient reached 0.75.

Figure 14 shows the spatial variations of the spatial and temporal clusters of the abnormally low marine primary productivity in the central Atlantic Ocean from June 2010 to March 2011.

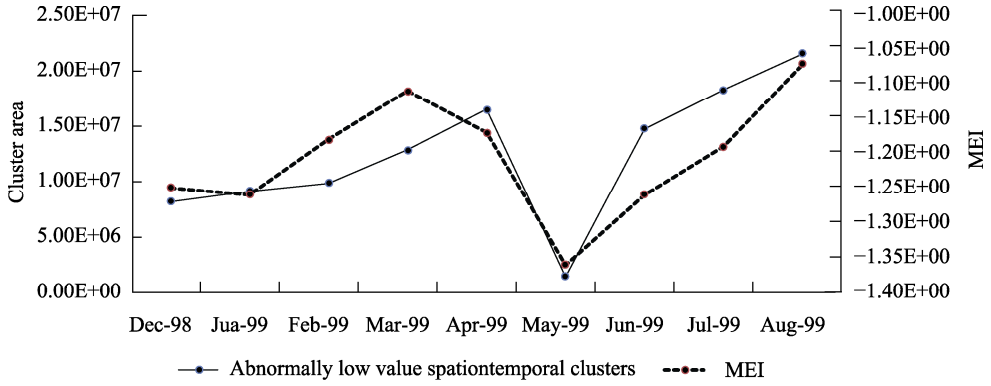

Figure 11 Correlation between the areas of the spatiotemporal clusters and MEI

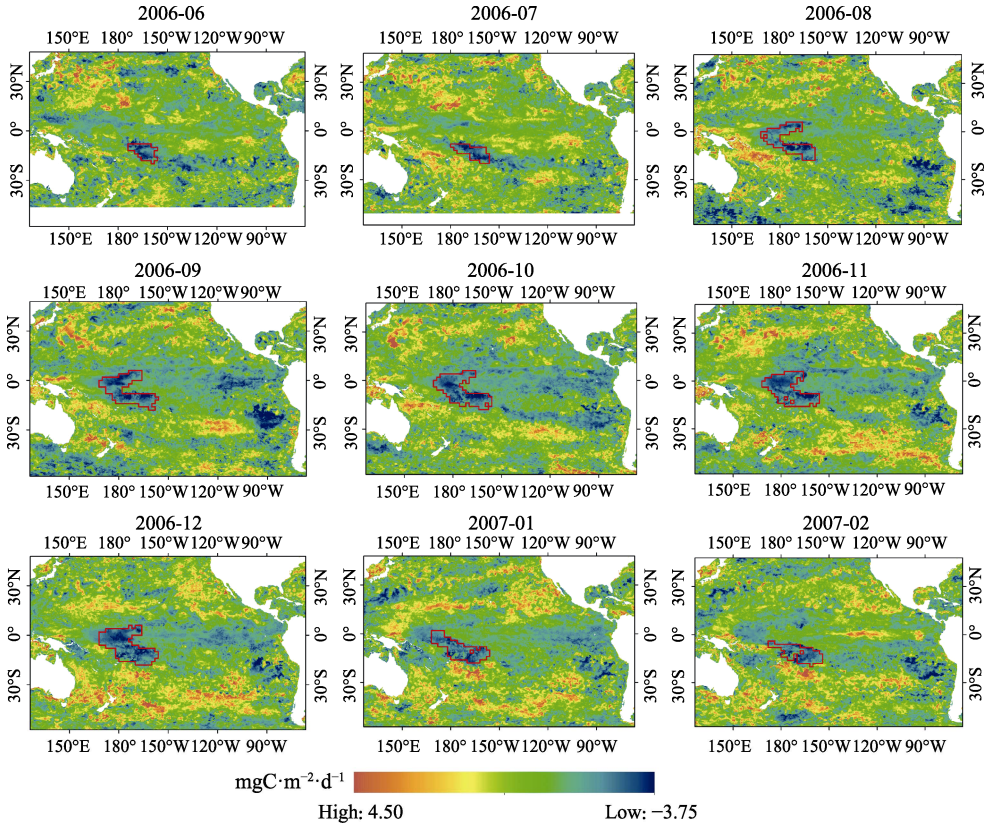

Figure 12 Spatial movement of the spatiotemporal clusters of the abnormally low values in the equatorial

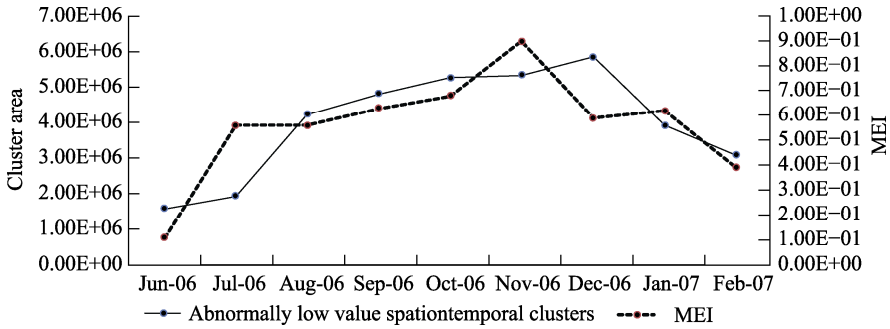

Figure 13 Correlation between the area of the spatiotemporal clusters and the MEI

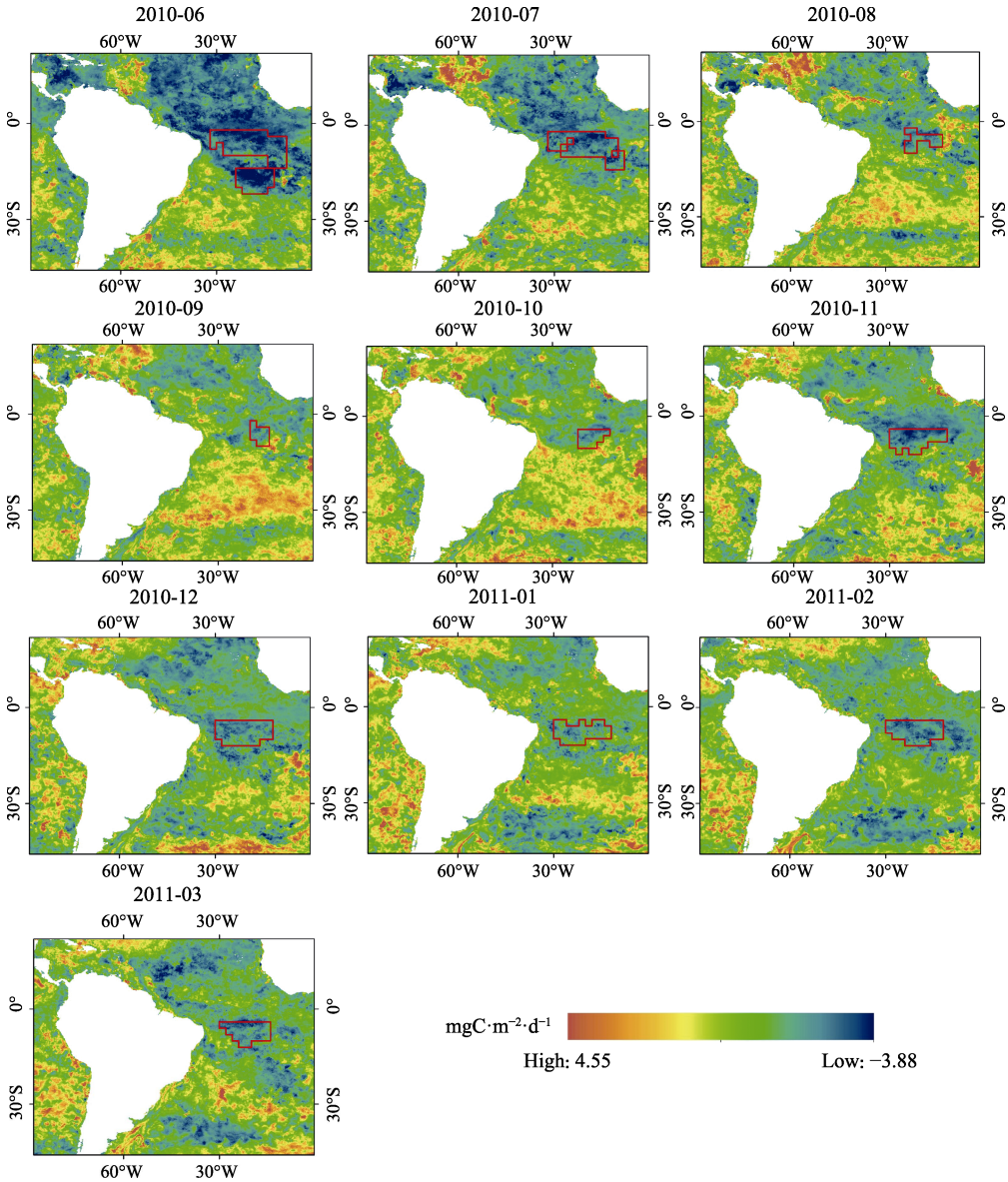

Figure 14 Spatial movement of the abnormally low-value spatiotemporal clusters in the central Atlantic Ocean

Over time, there is nearly no change in the location of the spatiotemporal abnormally low-value cluster, and the coverage area gradually became smaller. However, in November 2010, the area began to gradually increase and disappear. Figure 15 shows the correlation diagram between the area of the spatiotemporal evolution cluster and the MEI. It is seen that during El Niño, the spatiotemporal evolution cluster has a response relationship with the MEI index, and the correlation coefficient reached 0.63.

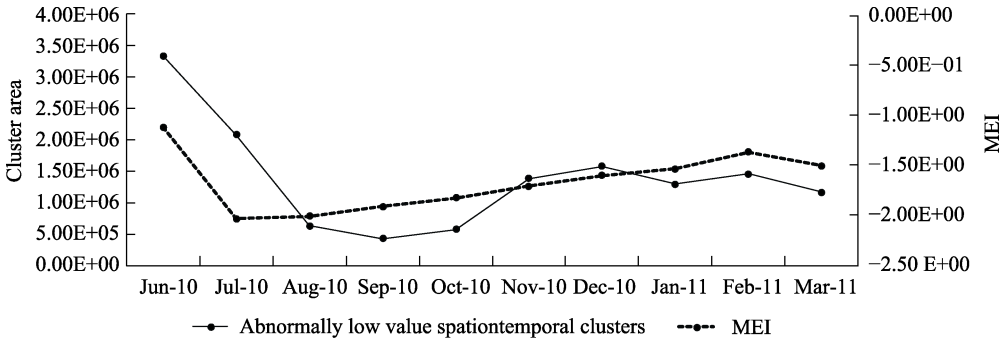

Figure 15 Correlation between the area of the spatiotemporal clusters and the MEI

5 Discussion and Summary

Based on the original datasets of the SeaWiFS and MODIS ocean primary productivity, this paper uses geographic spatiotemporal statistical methods to produce a dataset of standardized anomalies in marine primary productivity on three time scales from 1998 to 2019 with a data size of 16.82 GB. (4.81 GB in compression). The applicability of the MNPPAD dataset was verified using the coupling relationship between the abnormal change patterns of the marine primary productivity and ENSO events. In global seas, there is a strong correlation between the abnormal evolution clusters of the marine primary productivity and the MEI characterization. The results show that the abnormal change pattern of marine primary productivity is closely related to ENSO events, which provides an important data basis for global climate change research but is also necessary to increase the sample size to explore the relationship between abnormal change patterns of marine primary productivity and ENSO events. This is also the focus and direction of future research.

Author Contributions

Xue, C. J. and Hong, Y. L., made an overall design for the development of the dataset; Sun, Y. Q., and Xu, Y. F. collected and processed the raw data of marine primary productivity; Liu, J. Y. designed a method for mining anomalous changes in the spatio-temporal clusters of ocean; Hong, Y. L. and Sun, Y. Q. made data verification; Sun, Y. Q. wrote data paper.

Conflicts of Interest

The authors declare no conflicts of interest.

References

[1] Guosheng, L., Fang, W., Qiang, L., Jilong, L. Remote sensing inversion of primary productivity in the East China Sea and its spatiotemporal evolution mechanism [J]. *Acta Geographica Sinica*, 2003(4): 483–493.

[2] Peizhong, W. Satellite detection of marine primary productivity [J]. *Remote sensing of land and resources*, 2000(3): 7–15.

[3] Liu, J. Y., Xue, C. J., Fan, Y. G., *et al*. A grid-oriented space-attribute dual constrained clustering method [J]. *Journal of Geo-Information Science*, 2016, 19(4): 447–456. DOI:10.3724/SP.J.1047.2017.0447.

[4] Sun, Q., Xue, C. J., Liu, J. Y., *et al*. Mining and analysis of temporal and spatial correlation patterns between global marine primary productivity and marine environmental factors [J]. *Marine Environmental Science*, 2020, 39(3): 340–352. DOI: 10.13634/j.cnki.mes.2020.03.003.

[5] Behrenfeld, M. J., O'Malley, R. T., Siegel, D. A., *et al*. Climate-driven trends in contemporary ocean productivity [J]. *Nature*, 2006, 444: 752–755.

[6] Behrenfeld, M., Falkowski, P. A consumer's guide to phytoplankton primary productivity models [J]. *Limnology & Oceanography*, 1997, 42(7): 1479–1491.

[7] Bastos, A., Steven, W., Gouveia, C., *et al*. The global NPP dependence on ENSO: La Niña and the extraordinary year of 2011 [J]. *Journal of Geophysical Research*: *Biogeosciences*, 2013(118): 1247–1255. DOI: 10.1002/jgrg.20100.

[8] Chavez, F. P., Messie, M., Pennington, J. T. Marine primary production in relation to climate variability and change [J]. *Annual Review of Marine Science*, 2011, 3: 227–260.

[9] Messié, M., Chavez, F. A global analysis of ENSO synchrony: the oceans' biological response to physical forcing [J]. *Journal of Geophysical Research Oceans*, 2012, 117: C09001.

[10] Tal, Z., Zhou, X., Ma, S. Global ocean primary productivity remote sensing monitoring 9-km resolution monthly dataset based on ABPM model (2003–2012) [J/DB/OL]. *Digital Journal of Global Change Data Repository*, 2014. https://doi.org/10.3974/geodb.2014.02.03.V1.

[11] Wang, J. L., Zhang, Y. J., Yang, F., *et al*. Chlorophyll a concentration dataset of Poyang Lake (2009–2012) [J/DB/OL]. *Digital Journal of Global Change Data Repository*, 2014. https://doi.org/10.3974/geodb.2014.02.08.V1.

[12] Gao, S., Liu, W. H., Kang, J., et al. The 1-km resolution vegetation net primary productivity dataset for China and ASEAN in 2013 [J/DB/OL]. *Digital Journal of Global Change Data Repository*, 2015. https://doi.org/10.3974/geodb.2015.01.15.V1.

[13] Sun, Y. Q., Xue, C. J., Hong, Y. L., *et al*. Standardized anomaly dataset of global marine net primary productivity (1998–2019) [J/DB/OL]. *Digital Journal of Global Change Data Repository*, 2020. https://doi.org/10.3974/geodb.2020.07.13.V1. https://cstr.escience.org.cn/CSTR:20146.11.2020.07.13.V1.

[14] GCdataPR Editorial Office. GCdataPR data sharing policy [OL]. https://doi.org/10.3974/dp.policy.2014.05 (Updated 2017).

[15] Behrenfeld, M. J., Falkowski, P. G. Photosynthetic rates derived from satellite-based chlorophyll concentration [J]. *Limnology and Oceanography*, 1997, 42(1): 1–20.

[16] Couto, A., Holbrook, N., Maharaj, M. Unravelling eastern Pacific and central Pacific ENSO contributions in south Pacific chlorophyll-a variability through remote sensing [J]. *Remote Sensing*, 2013, 5(8): 4067–4087.

[17] Zhang, P., Steinbach, M., Kumar, V., *et al*. Discovery of Patterns of Earth Science Data Using Data Mining [M]. In New Generation of Data Mining Applications (Zurada, J., Kantardzic, M., eds), New Jersey: John Wiley & Sons Inc., 2005.

[18] Xue, C., Song, W., Qin, L., *et al*. A spatiotemporal mining framework for abnormal association patterns in marine environments with a time series of remote sensing images [J]. *International Journal of Applied Earth Observation and Geoinformation*, 2015, 38: 105–114.

[19] Liu, J., Xue, C., He, Y., *et al*. Dual-constraint spatiotemporal clustering approach for exploring marine anomaly patterns using remote sensing products [J]. *IEEE J-STARS*, 2018, 11(11): 3963–3976.